ACI STRUCTURAL JOURNAL TECHNICAL PAPER

Title no. 106-S84

Bond Behavior of Reinforcing Bars in Tensile Strain-Hardening Fiber-Reinforced Cement Composites

by Shih-Ho Chao, Antoine E. Naaman, and Gustavo J. Parra-Montesinos

Bond between deformed reinforcing bars and concrete induces significant tensile stresses that lead to cracking in concrete due to its weak and brittle nature in tension. Contrary to plain concrete and conventional fiber-reinforced concrete, high-performance fiber-reinforced cement composites (HPFRCCs) show strain-hardening response under tension and, thus, their use can lead to enhanced bond performance. Pullout-type tests comprising various types of loadings were carried out to investigate the influence of strain-softening and strain-hardening fiber-reinforced cementitious (FRC) composites on the bond strength and the bond stress-slip response of deformed reinforcing bars. Test results showed that the bridging effect provided by fibers in FRC composites after cracking can effectively provide post-cracking tensile capacity to the concrete matrix and limit crack width, thereby leading to enhanced bond resistance. HPFRCC specimens gave the best bond performance in terms of bond strength and stiffness retention capacity, as well as damage-control ability.

Keywords: bond stress; development length; fiber-reinforced cementitious composites; high-performance cement composites; pullout; strain.

INTRODUCTION

Composite action between concrete and reinforcing steel cannot occur without bond. Therefore, the bond performance of reinforcing bars plays a major role in the behavior of reinforced concrete structures when subjected to static and dynamic loads. Insufficient bond can lead to a significant decrease in the load-carrying capacity and stiffness of the structure when subjected to monotonic, cyclic, or reversed cyclic loading. Aspects pertaining to bond behavior in reinforced concrete members include strength development, development length, anchorage of reinforcement, bar splicing, and ductility under monotonic and reversed cyclic loading.

The bond resistance of reinforcing bars embedded in concrete depends primarily on frictional resistance and mechanical interlock. The chemical adhesion bond, if any, fails at very small slips. Frictional bond provides initial resistance against loading and further loading mobilizes the mechanical interlock between the concrete and bar ribs. Mechanical interlock leads to inclined bearing forces, which in turn lead to transverse tensile stresses and internal inclined splitting (bond) cracks along reinforcing bars. These cracks, commonly referred to as Goto cracks (Goto 1971) or conical cracks, lead to a reduction in bond strength and, should their width become significant, to a progressive deterioration of bond. Further, when these tensile splitting cracks become wider and reach the concrete surface, bond resistance drops significantly, or is completely lost. For reinforcing bars subjected to reversed cyclic loading, the opened inclined cracks also cause significant deterioration in bond stiffness and strength due to the presence of gaps between the steel ribs and adjacent concrete (Viwathanatepa et al. 1979). Hence, the tensile strength and strain capacity of concrete are major factors affecting bond behavior.

Lateral confinement is an effective way to restrain the widening and propagation of cracks, thus leading to increased bond resistance. A relatively large amount of transverse reinforcement is needed, however, to prevent the opening and propagation of splitting cracks in regions of members/structures where bond demand is high, such as in beam-column joints of framed structures subjected to unbalanced moments and anchorage zones of prestressed concrete beams. This leads to congestion of reinforcement, and thus construction/manufacturing of such regions of members becomes difficult, costly, and requires close quality control.

In recent years, considerable attention has been paid to fiber-reinforced concrete or fiber- reinforced cementitious (FRC) composites, in particular those referred to as high-performance fiber-reinforced cement composites (HPFRCCs). Figure 1 illustrates the typical tensile stress-strain responses of conventional and high-performance FRC materials (Naaman 2003), in which ε_{cc} and σ_{cc} are the composite tensile strain and strength at first cracking, respectively, and ε_{pc} and σ_{pc}

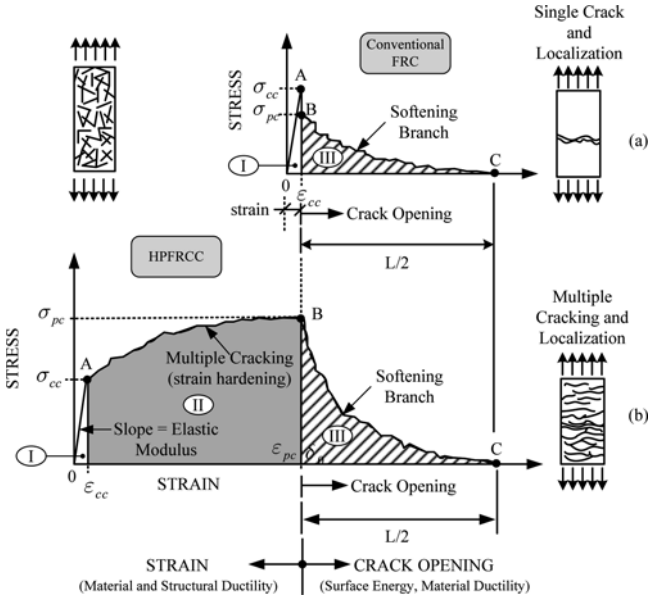

Fig. 1—Stress-strain response of conventional FRC and HPFRCC (Naaman 2003).

ACI Structural Journal, V. 106, No. 6, November-December 2009.
MS No. S-2009-001 received January 3, 2009, and reviewed under Institute publication policies. Pertinent discussion including author's closure, if any, will be published in the July-August 2010 *ACI Structural Journal* if the discussion is received by March 1, 2010.

ACI member **Shih-Ho Chao** *is an Assistant Professor in the Department of Civil Engineering at the University of Texas at Arlington, Arlington, TX. He received his PhD in civil engineering from the University of Michigan, Ann Arbor, MI. He is a member of ACI Committee 544, Fiber Reinforced Concrete, and Joint ACI-ASCE Committees 352, Joints and Connections in Monolithic Concrete Structures, and 408, Development and Splicing of Deformed Bars. His research interests include fiber-reinforced concrete, prestressed concrete, and seismic behavior of structural members.*

Antoine E. Naaman, *FACI, is Professor Emeritus in the Department of Civil and Environmental Engineering at the University of Michigan. He is a member of ACI Committees 363, High-Strength Concrete; 440, Fiber Reinforced Polymer Reinforcement; 544, Fiber Reinforced Concrete; 549, Thin Reinforced Cementitious Products and Ferrocement; and Joint ACI-ASCE Committees 343, Concrete Bridge Design, and 423, Prestressed Concrete. His research interests include high-performance fiber-reinforced cement composites and prestressed concrete.*

ACI member **Gustavo J. Parra-Montesinos** *is an Associate Professor of civil and environmental engineering at the University of Michigan. He is Secretary of ACI Committee 335, Composite and Hybrid Structures, and a member of ACI Committees 318, Structural Concrete Building Code, and 544, Fiber Reinforced Concrete, and Joint ACI-ASCE Committee 352, Joints and Connections in Monolithic Concrete Structures. His research interests include the seismic behavior and design of reinforced concrete, hybrid steel-concrete, and fiber-reinforced concrete structures.*

are the composite peak post-cracking tensile strain and strength, respectively. The responses of the two materials have a similar initial ascending portion (0A). After first cracking, however, the HPFRCC material shows a hardening portion (AB) up to relatively high strains, typically higher than 0.5% (that is, exceeding two times the yield strain of a typical reinforcing bar), whereas the regular FRC material exhibits a rapid strength decay, generally described as strain-softening. Moreover, after first cracking, multiple cracks develop throughout the HPFRC composite, as opposed to a single localized crack in regular FRC composites. This unique portion (AB) for HPFRCCs describes their strain-hardening behavior, which leads to the large material toughness and their classification as strain-hardening FRC composites. Today, such performance can be achieved by using relatively lower fiber volume fractions compared to earlier versions of HPFRCCs (between 1.5 and 2%, rather than 5 to 9%) through proper selection of matrix constituents and fiber parameters, as well as proper mixing.

In view of their superior tensile response, the use of strain-hardening FRC composites is likely to substantially enhance bond behavior in reinforced concrete structures, especially by preventing wide splitting cracks from opening should they occur. A host of additional benefits can be offered by using HPFRC composites, particularly as replacement of confinement reinforcement in critical regions of earthquake resistant structures (Parra-Montesinos 2005).

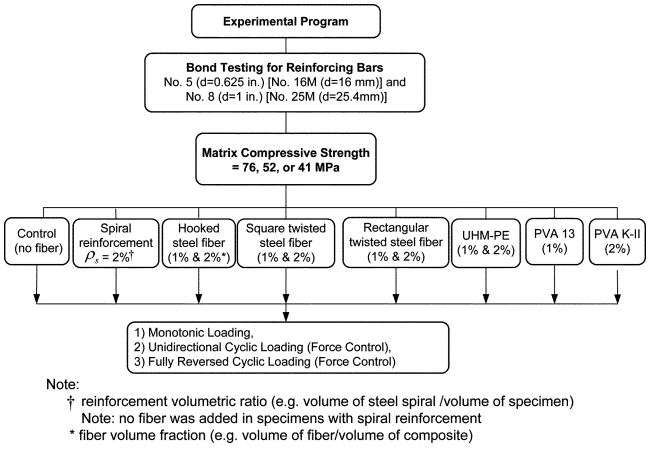

Fig. 2—Flowchart of testing program. (Note: 1 mm = 0.04 in.; 1 MPa = 0.145 ksi.)

RESEARCH SIGNIFICANCE

Bond failure is generally brittle due to the brittle tensile behavior of concrete. An appreciable improvement in bond can be anticipated by substituting conventional concrete with an FRC composite, particularly one with tensile strain-hardening behavior. The experimental program described herein focuses on evaluating the bond stress versus slip response of deformed reinforcing bars embedded in an FRC composite obtained through direct pullout-type tests. The bond stress versus slip relationship of the interface between a bar and its surrounding matrix can be considered the constitutive property of the interface. It gives a complete description of the bond resistance at any given slip, thus allowing the measurement of the maximum bond stress, bond modulus, average bond stress over a given slip, and shear-friction energy (pullout work) up to any given slip.

EXPERIMENTAL PROGRAM

Test parameters and test setup

The overall experimental program, aimed at evaluating bond between reinforcing bars and FRC composites, is described in Fig. 2. All pullout specimens consisted of a reinforcing bar embedded in either a plain concrete (control) or FRC prism having a dimension of 150 x 150 x 102 mm [6 x 6 x 4 in.] (bar embedment of 102 mm [4 in.]). The prismatic specimen was supported at its eight corners by 50 x 38 x 13 mm [2 x 1.5 x 0.5 in.] plates, as illustrated in Fig. 3. The reinforcing bars used (No. 16M and No. 25 M [No. 5 and No. 8]) had a nominal tensile strength of 420 MPa (60 ksi). These bars were threaded at their ends and attached to the test setup through nuts; only the nut position needed to be changed for different loading conditions. Details of the test setup can be found elsewhere (Hota and Naaman 1997; Chao 2005; Chao et al. 2006). The test parameters included fiber type, fiber volume fraction, fiber length, and loading type (Fig. 2). Twelve series of specimens were tested following three types of loading: 1) monotonic loading; 2) unidirectional cyclic loading (force control); and 3) fully reversed cyclic loading (force control). At least two specimens for each parameter in each series were tested. It should be noted that steel spiral reinforcement (f_y = 207 MPa [30 ksi]; f_u = 317 MPa [46 ksi]) at a volumetric ratio of 2% was used as conventional confinement in one of the series.

It is important to note that ACI Committee 408 (2003) suggests that to achieve a representative stress state in a bond test, the compressive forces must be located away from the reinforcing steel at least a distance approximately equal to the embedded length of the steel within the concrete. This is due to the fact that conventional pullout-type bond tests using bearing plates, while placing the steel in tension, result in compressive forces on the concrete. In most reinforced concrete members, however, both the steel and surrounding concrete are subjected to tension. In the test setup used in this study, no bearing plate was used for pulling the bars through, thus minimizing the confinement effect in the loading direction. In addition, the effect of concrete compressive forces on bond behavior was minimized by keeping the reinforcing bar apart from the compressed concrete zone a distance approximately equal to the embedded length of the bar (102 mm [4 in.] refer to Fig. 3). Moreover, because small gaps existed between the specimen and the test setup, no lateral

contact (thus no confinement) occurred even when cracks developed. This was true for all the fiber-reinforced concrete specimens. However, for the control plain concrete specimens, which had no transverse reinforcement, some confinement developed once very wide cracks formed due to splitting of the concrete.

Slip data were recorded using a pair of linear variable differential transformers (LVDTs), while the applied load was monitored through a load cell. Because the bars behaved elastically and the embedment length was short (102 mm [4 in.]), the slip values at the unloaded and loaded bar ends did not differ significantly from each other should bar elastic deformations outside the embedded portion be ignored (approximately 0.1 mm [0.004 in.] for a typical maximum load). Therefore, the measured slip was considered to represent the average local slip in the middle of the embedded length with sufficient accuracy. The average bond stress between the reinforcing bar and the surrounding concrete σ was calculated as

$$\sigma = P/(p_{ps}L) \quad (1)$$

where P is the applied load (kN); L is the embedment length (102 mm [4 in.]); and p_{ps} is the bar perimeter, equal to πd, where d is the nominal diameter of the reinforcing bar.

FRC composite material properties

The matrix composition and average compressive strength for the FRC composites used in this study are listed in Table 1. Note that the addition of fibers in volume fractions between 1 and 2% into cement matrixes did not significantly affect the matrix compressive strength. The compressive strength shown is the average compressive strength of all specimens made with a particular mixture, including both plain concrete and FRC composites. Five types of fibers were used, namely, ultra-high molecular weight polyethylene (UHM-PE) fibers, polyvinyl alcohol (PVA) fibers (PVA 13 and PVA K-II), hooked steel fibers, and twisted polygonal steel fibers. Table 2 summarizes the fiber properties. The twisted steel fiber has twisted ribs, which create a very effective mechanical bond along the entire fiber length. Unlike conventional steel fibers, when being pulled out from a cement matrix, twisted steel fibers can maintain a high level of resistance up to slips representing 70 to 80% of the embedded length (Sujivorakul 2002). Twisted steel fibers with either square or rectangular cross sections, as well as two different aspect ratios, were used in this investigation (Table 2).

Results from direct tension tests on 560 mm (22 in.) long dog-bone-shaped specimens with a 25 x 50 mm (1 x 2 in.) cross section over a 200 mm (8 in.) gauge length (Fig. 4(a)) yielded the typical stress-strain curves shown in Fig. 4(b) for the FRC composites. As can be seen, the specimen with 2% volume fraction of twisted steel fibers exhibited a tensile strain-hardening behavior up to approximately 0.6% strain with a peak strength close to 11.7 MPa (1.7 ksi), which in turn led to the formation of multiple cracks, as shown in Fig 4(d). Figure 4(b) shows that, with the same fiber volume fraction (2%), the composite with hooked steel fibers exhibited a tensile hardening response up to only 0.2% strain. Thereafter, the stress decay was gradual, and the FRC composite maintained approximately 50% of the peak strength at a tensile strain of 1%. FRC composites with UHM-PE fibers exhibited a

Table 1—Relative composition of matrix mixtures by weight and average compressive strength

Matrix	Cement, Type III	Fly ash	Sand*	Silica fume	High-range water-reducing admixture	Water	f_c', MPa
Mixture 1	0.8	0.2	1.0	0.07	0.04	0.26	76
Mixture 2	1.0	0.15	1.0	—	—	0.40	52
Mixture 3	0.8	0.2	1.0	—	—	0.45	41

*Flint sand ASTM 50-70.
Note: 1 MPa = 0.145 ksi.

Table 2—Properties of fibers

Fiber type	Diameter, mm	Length, mm	Density, g/cc	Tensile strength, MPa	Elastic modulus, GPa
UHM-PE	0.038	38	0.97	2585	117
PVA 13	0.19	13	1.31	900	29
PVA K-II*	0.04	8	1.31	1600	40
Steel hooked	0.55	30	7.9	1100	200
Rectangular twisted†	0.3‡	30	7.9	2570	200
Square twisted†	0.3‡	30 and 20	7.9	2750	200

*Surface is oiled (oiling content equals 0.8% by weight) to reduce chemical bond.
†Five ribs per cm,
‡Equivalent diameter.
Note: 1 mm = 0.04 in.; 1 MPa = 0.145 ksi; 1 GPa = 145 ksi; 1 g/cc = 62.4 pcf.

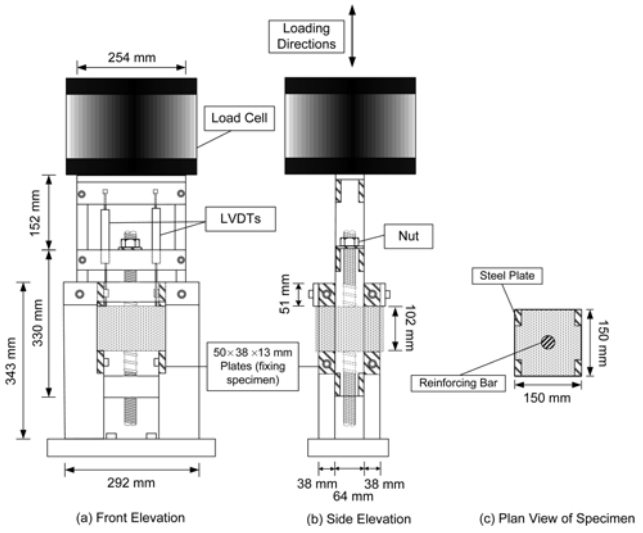


(d) Specimen under Test

Fig. 3—Test setup and specimen geometry. (Note: 1 mm = 0.04 in.)

behavior similar to that with hooked steel fibers, but with a longer strain-hardening plateau, whereas FRC composites with PVA fibers showed the lowest tensile strength and strain capacity (Fig. 4(c)). Tension tests for the FRC composites with 1% fiber by volume were not systematically carried out for this program. Limited earlier tests showed, however, a tensile softening response in composites with 1% volume fraction of either UHM-PE, PVA or hooked steel fibers, whereas a strain-hardening behavior was observed in composites with 1% volume fraction of twisted steel fibers (Sujivorakul 2002).

RESULTS FROM EXPERIMENTAL PROGRAM

Before describing the results from the experimental program in detail, a brief discussion of the bond mechanisms developed in reinforcing bars embedded in strain-hardening FRC composites is warranted.

Observed bond mechanism of reinforcing bars embedded in HPFRC composite materials

As mentioned previously, bearing forces induced by mechanical interlocking between a deformed reinforcing bar and surrounding concrete often lead to inclined cracks in the concrete matrix. Upon further tension, these internal inclined cracks grow wider and extend longer, leading to large residual slip. If no transverse reinforcement is present, circumferential tensile stress caused by the radial component of the bearing forces would lead to the formation of splitting cracks and ultimately to a bond failure (refer to Fig. 5(a)). If significant transverse reinforcement is present, however, the propagation and widening of these cracks can be controlled. In this case, degradation of bond strength and stiffness would be mainly caused by concrete crushing at the toe of the bar ribs and shearing off of the concrete between the ribs, although a splitting type failure could still eventually occur. A detailed description of the bond resistance mechanism for confined reinforced concrete under monotonic and cyclic loading can be found elsewhere (Orangun et al. 1977; Viawathanatepa et al. 1979; Eligehausen et al. 1983).

In HPFRC composites, the fiber bridging effect helps control the crack opening and propagation, thus increasing bond strength. After initial cracking and upon increased bar pullout load, the radial compression exerted on the concrete by the bar ribs is redistributed to the whole matrix due to the presence of fibers. Multiple fine cracks form at this stage; the strain-hardening characteristics of the FRC control the widening of these cracks with no (or little) bond strength deterioration (Fig. 5(b)). In general, everything else being the same, it has been observed that specimens with multiple cracking exhibit higher bond resistance. This is due to the fact that the stress is redistributed and more than one cracked section participates in resisting the tensile stresses induced by the bearing forces (refer to Fig. 5(c)). Upon further slippage, following the initial pullout of fibers, longitudinal cracks along the bar axis develop; this corresponds approximately to the time at which the maximum bond strength is attained. Further widening and propagation of the internal inclined bond cracks and of the longitudinal cracks are hindered by the fibers. If the fibers can effectively bridge the longitudinal cracks without excessive opening, the matrix around the bar ribs will be eventually crushed under increasing bar slip. Thus, the use of a strain-hardening FRC composite will give rise to higher bond stress at a given slip in both the ascending and the descending branches of a bond stress-slip curve (Fig. 5(d)).

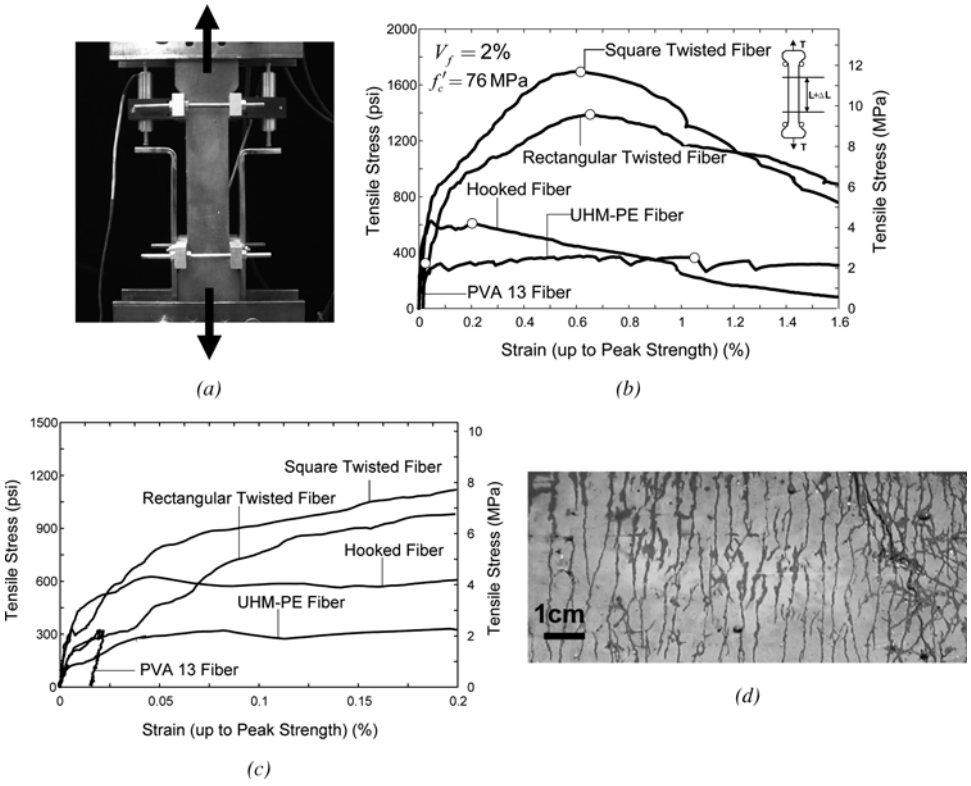

Fig. 4—(a) Material tensile test setup; (b) typical tensile stress-strain behavior of cementitious composites; (c) enlargement of initial portion of tensile stress-strain curves; and (d) multiple cracking of tensile specimens with twisted fibers. (Note: 1 cm = 0.0394 in.)

Monotonic loading

Figures 6 and 7 show the typical monotonic average bond stress-versus-slip responses of bars embedded in specimens with various fibers at 1 and 2% volume fraction (only specimens with 76 MPa (11 ksi) matrix compressive strength are shown), respectively. Figure 6(b) shows an enlarged portion of Fig. 6(a), up to 5 mm (0.2 in.) slip, to clearly highlight the ascending branch. In addition, the pullout responses observed in bars embedded in plain concrete and in a concrete prism confined by steel spiral reinforcement are shown in the same figures for comparison. The bond stress (average of two identical specimens) at maximum load (bond strength) for all specimens tested in this study is listed in Table 3. The control specimen, without any reinforcement, exhibited a low bond strength (1.5 MPa [0.22 ksi]) and a brittle behavior after splitting cracks formed at a slip of approximately 0.3 mm (0.012 in.).

At a fiber volume fraction of 1%, all test specimens showed improved pullout response compared to the control specimen. Under monotonic loading, the specimens with UHM-PE fibers exhibited the highest bond strength (10.1 MPa [1.45 ksi]), whereas specimens with PVA 13 fibers showed the lowest bond strength (5 MPa [0.73 ksi]). Specimens with either other types of fibers or a 2% volumetric ratio of spiral reinforcement generally reached approximately the same peak bond stress (approximately 7.5 MPa [1.1 ksi]). With spiral reinforcement, however, significant damage in terms of concrete spalling and a cone-shaped fracture occurred just after the peak load (refer to Fig. 8(b)).

When fiber volume fraction was low (1%), the role that fiber length played was more noticeable, as observed from specimens with square twisted steel fibers (20 and 30 mm [0.8 and 1.2 in.] long, with same equivalent diameter). This

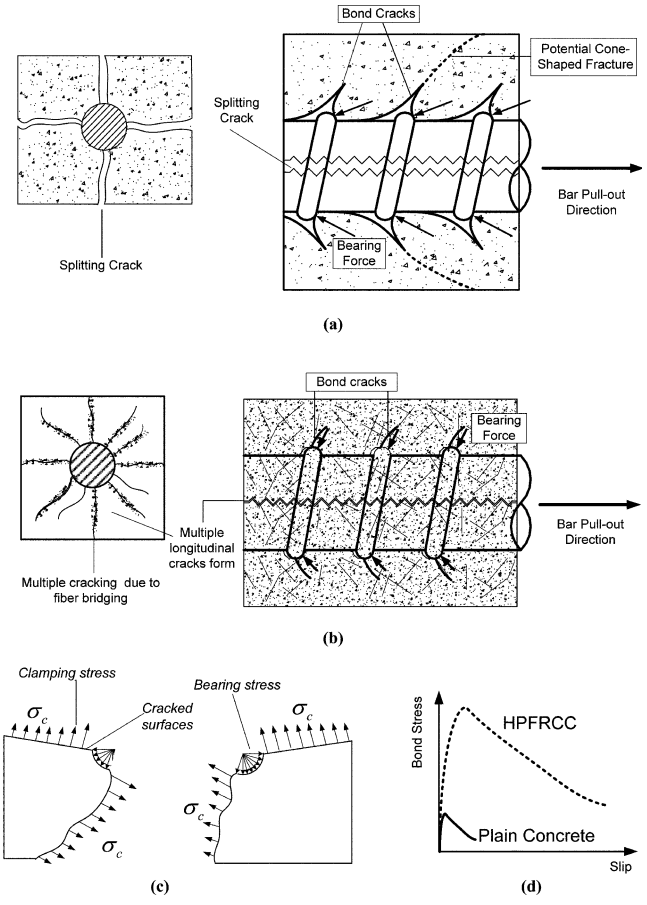

Fig. 5—Bond mechanisms of reinforcing bar in: (a) conventional concrete; (b) HPFRCC; (c) clamping stress due to fiber bridging in specimens in multiple cracking; and (d) typical bond stress-slip responses.

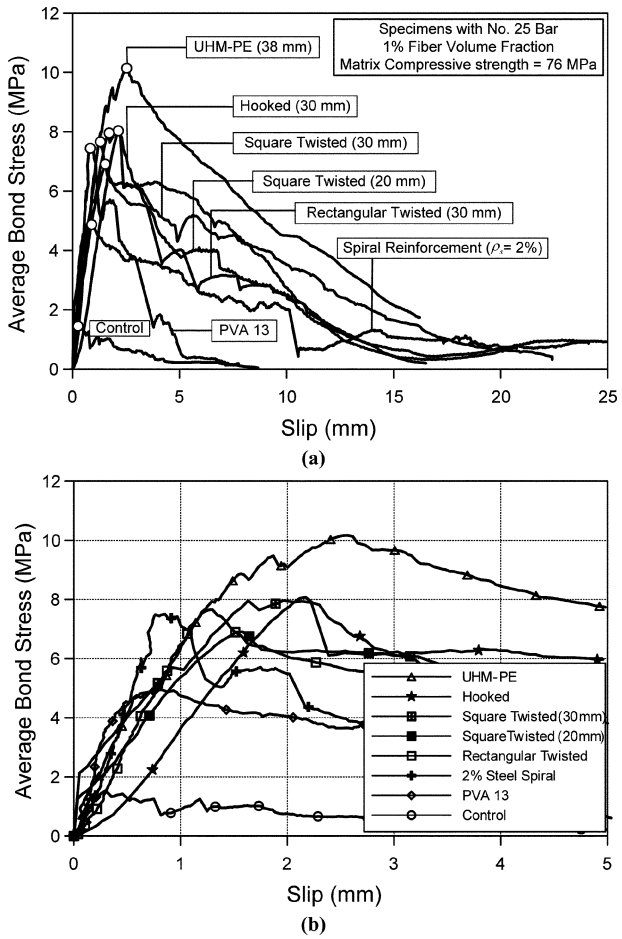

Fig. 6—(a) Comparison of bond stress-slip behavior of specimens with 1% fiber volume fraction; (b) enlargement of ascending portion of curves. (Note: 1 mm = 0.04 in.; 1 MPa = 0.145 ksi.)

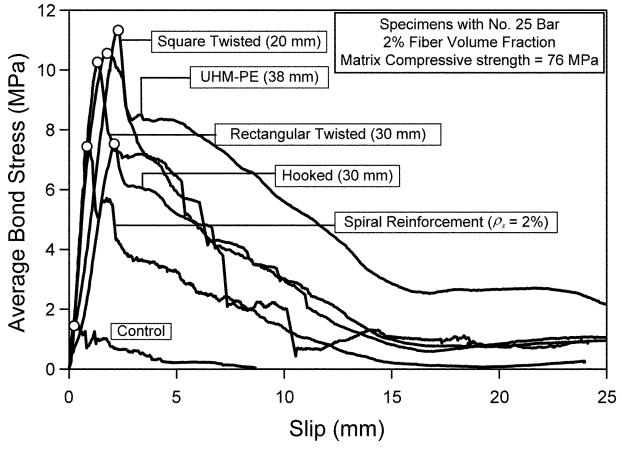

Fig. 7—Comparison of bond stress-slip behavior of specimens with 2% fiber volume fraction. (Note: 1 mm = 0.04 in.; 1 MPa = 0.145 ksi.)

could be explained by the fiber-reinforcing index F, which is defined as follows (Naaman and Reinhardt 1996)

$$F = \tau \times V_f \times (l/d_f) \quad (2)$$

where τ is the average bond strength at the fiber-matrix interface, V_f is the fiber volume fraction, l is the fiber length, and d_f is the fiber diameter.

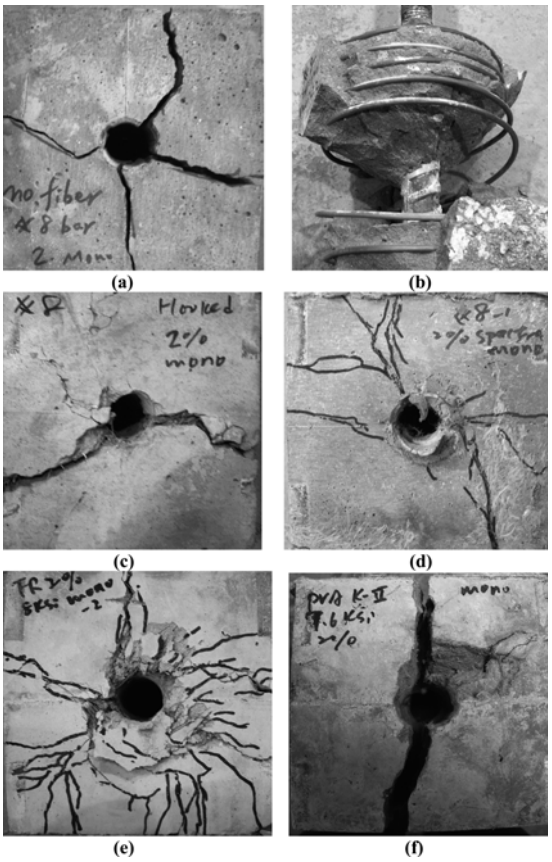

Fig. 8—Cracking pattern in test specimens with various reinforcements under monotonic loading (No. 25M bar). Specimen with: (a) no fiber; (b) 2% spiral reinforcement; (c) 2% hooked steel fiber; (d) 2% UHM-PE fiber; (e) 2% rectangular steel twisted fiber; and (f) 2% PVA K-II fiber.

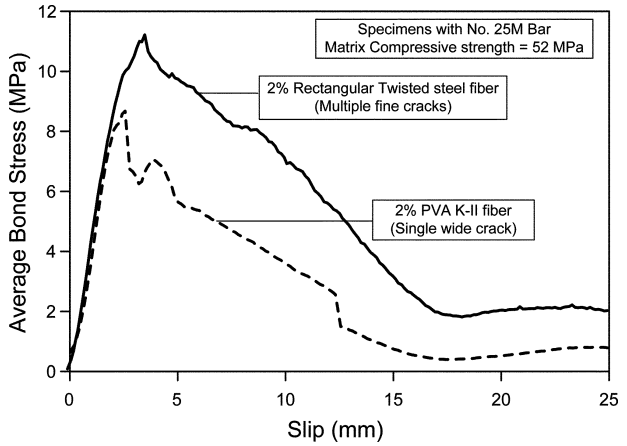

Fig. 9—Typical bond stress-slip responses of specimens with 52 MPa (7.5 ksi) matrix compressive strength. (Note: 1 mm = 0.04 in.; 1 MPa = 0.145 ksi.)

If a reinforcing bar is pulled out from a matrix, the cracks need to open for the bar to move through. As a consequence, the longer fiber offers better bridging resistance due to longer embedded length, thus increasing the bar bond strength. For short fibers, however, this drawback can be compensated by increasing the fiber volume to 2%.

It is noted that, with the same fiber volume fraction, the number of UHM-PE fibers per unit volume of composite is approximately 50 times that of twisted steel fibers. This large number of UHM-PE fibers can more effectively hinder the extension and expansion of cracks, thus leading to multiple fine cracks and better bond characteristics, even at low fiber volume fractions. Nevertheless, it can be shown through Eq. (2) that twisted steel fibers give higher bridging efficiency than UHM-PE fibers. Assuming the same fiber volume fraction (1%), the calculated fiber reinforcing index is 930 and 630 for twisted steel and UHM-PE fibers, respectively (based on previous studies: $\tau_{Twisted} \approx 9.3$ MPa [1.35 ksi] [Chao 2005] and 0.63 MPa [0.09 ksi] [Li et al. 1996]). This explains the better performance of twisted steel fiber specimens in spite of the smaller fiber number compared with the UHM-PE fiber specimens.

Under monotonic loading, no significant improvement in bar bond strength was observed when the fiber volume fraction was increased from 1 to 2% for hooked steel fiber and UHM-PE fiber specimens (refer to Fig. 6 and 7). On the other hand, peak bar bond stress was significantly increased by doubling the amount of twisted steel fibers, from 1 to 2% by volume. This increase in bond strength was approximately 60% for the square twisted steel fiber specimens and 40% for the rectangular twisted steel fiber specimens. The specimens with square twisted steel fibers (20 mm [0.8 in.] long) exhibited the highest bar bond stress (11.3 MPa [1.64 ksi]). It is believed that the superior bond properties of twisted steel fibers were responsible for that improvement. It should be mentioned that with the same specimen geometry, a peak bond strength of 9.6 MPa (1.4 ksi) was reported for reinforcing bars embedded in slurry-infiltrated fiber concrete (SIFCON)

Table 3—Monotonic peak bond stress of specimens with various types of fibers or reinforcement

Fiber/ reinforcement		No. 25 bar			No. 16 bar
	Matrix compressive strength	76 MPa	52 MPa	41 MPa	76 MPa
	Fiber or reinforcement content	Peak bond stress, MPa			
Control (no fiber or reinforcement)	0%	1.5	—	—	4.6
Square twisted, 20 mm	1%	6.9	—	—	—
	2%	11.3	—	—	—
Square twisted, 30 mm	1%	8.0	—	—	—
Rectangular twisted, 30 mm	1%	7.7	—	—	12.3
	2%	10.3	11.0	8.9	14.4
UHM-PE	1%	10.1	—	—	15.1
	2%	10.6	—	—	16.2
Hooked	1%	8.0	—	—	—
	2%	7.7	—	—	—
PVA 13	1%	5.0	—	—	—
PVA K-II	2%	—	8.6	—	—
Steel spiral	$\rho_s = 2\%$	7.5	—	—	—

Note: 1 mm = 0.04 in.; 1 MPa = 0.145 ksi.

with 9.7% volume fraction of hooked steel fibers (Hota and Naaman 1997). Compared with the specimens with 2% volumetric ratio of spiral reinforcement, the specimens with 2% volume fraction of square twisted steel fibers showed 50% greater bond strength. In general, increasing the fiber amount from 1 to 2% led to a reduction in crack width and damage at large slips, and the use of tensile strain-hardening FRC composites (that is, UHM-PE or twisted steel fiber specimens; refer to Fig. 4(b)) led to better bar bond performance.

Other observations

FRC composite specimens with matrix compressive strengths of 41 and 52 MPa (6 and 7.5 ksi) showed similar behavior (that is, shape of the bond stress-versus-slip curve) as the specimens with 76 MPa (11 ksi) compressive strength. Typical bond stress-slip responses of specimens with 52 MPa (7.5 ksi) matrix strength are shown in Fig. 9. It is noted that for specimens with PVA K-II fibers, there was a sudden drop in bond strength due to the formation of a wide splitting crack (Fig. 8(f)). This bond strength loss was followed by a slight strength increase due to rotation of the specimen around this crack, which led to locking of the bar. It was also observed that, due to the slightly weaker matrix tensile strength, specimens with 52 MPa (7.5 ksi) matrix showed more multiple cracking than specimens with 76 MPa (11 ksi) matrix, which in turn led to higher bond resistance. Further reduction in the matrix strength resulted in a decrease in the bond strength even though multiple cracking formed, as observed in the specimens with 41 MPa (6 ksi) matrix strength.

Specimens with No. 16M (No. 5) bars exhibited similar responses as specimens with No. 25M (No. 8) bars. Cracks were much narrower in the smaller bar specimens, however. In addition, as shown in Table 4, the peak bond stress ratio between No. 16M and No. 25M (No. 5 and No. 8) bar specimens was approximately equal to the inverse of their diameter ratio, regardless of fiber type. This trend is consistent with the ACI development length expression (ACI 318-08, Eq. (12-1)[ACI Committee 318 2008]).

ACI Committee 408 (2003) has suggested that bond strength is generally proportional to $f_c'^{1/4}$ for bars without transverse reinforcement confinement. In general, this relation seems reasonable for FRC elements without transverse reinforcement, based on the observation from this study (Chao 2005). Further experimental work, however, is required to reach a definite conclusion in this regard.

Cracking patterns

Figure 8 shows the cracking patterns for selected specimens after testing. The control specimens exhibited severe cracking and splitting, whereas the 2% spirally reinforced specimens exhibited cracking and a cone-shaped fracture. In contrast, the specimens with UHM-PE and twisted steel fibers (Fig. 8(d) and (e)) showed appreciable damage tolerance and maintained their integrity throughout the test due to the fiber bridging effect, which prevented cracks from opening widely. The specimen with PVA K-II fibers, on the other hand, exhibited a brittle bond failure, as shown in Fig. 8(f). It should be noted that only the cracks visible to the naked eye were marked.

Unidirectional cyclic loading

Unidirectional, force-controlled cyclic loading tests were conducted to investigate the bond strength and stiffness retention capacity of reinforcing bars embedded in FRC composites. The applied loading history, shown in Fig. 10(a), was based on the monotonic bond stress-slip response, which can be considered an envelope response for this type of loading (Balaguru et al. 1996). The application of cyclic loading typically leads to increasing residual slip with increasing number of cycles. This occurs because the reinforcing bar faces an increasingly damaged matrix and gradually wider and larger cracks. Fiber or steel spiral confinement delays this process.

Typical results from the unidirectional force-controlled cyclic tests are shown in Fig. 11. The slight noise in the responses was due to limitations in the recording instrumentation.

Table 4—Relation between peak bond stress and bar diameter (UHM-PE and rectangular twisted fibers)

Fiber type	Bar	Average peak bond stress, MPa	Bond strength ratio, No. 16/No. 25	Bond diameter ratio, No. 25/No. 16
1% UHM-PE	No. 25M	10.1	1.5	1.6
	No. 16M	15.1		
2% UHM-PE	No. 25M	10.6	1.5	1.6
	No. 16M	16.2		
1% rectangular twisted	No. 25M	7.7	1.6	1.6
	No. 16M	12.3		
2% rectangular twisted	No. 25M	10.3	1.4	1.6
	No. 16M	14.4		

Note: 1 MPa = 0.145 ksi.

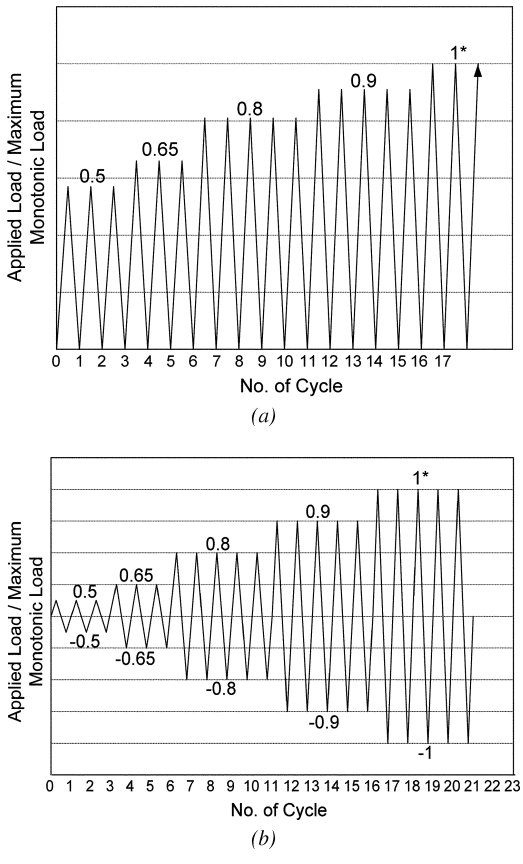

Fig. 10—Loading protocol for: (a) unidirectional loading (force-controlled tests) (note: if peak monotonic bond strength could not be attained, then specimen was monotonically loaded until failure; and (b) reversed cyclic loading (forced-controlled tests).

As can be seen, the bond performance of the specimen reinforced with conventional spiral reinforcement ($\rho_s = 2\%$) was not as good as that of the specimen with twisted steel fibers (and HPFRC composite specimens in general); its maximum bond stress level was approximately 40% smaller. The bond stiffness of the spirally reinforced specimen degraded considerably after 10 cycles, while good bond stiffness retention was observed for up to 25 cycles for the HPFRCC specimens (both UHM-PE and twisted steel fiber specimens). Severe spalling and fracturing of concrete contributed to the inferior bond performance of specimens with spiral reinforcement. For the specimens with twisted steel fibers, the residual slip was only approximately 0.4 mm (0.016 in.) after 25 loading cycles.

Fully reversed cyclic loading

Bond deterioration usually occurs in reinforcing bars of concrete members when subjected to fully reversed cyclic loading, even when substantial confinement reinforcement is present (Viawathanatepa et al. 1979). This is due to the concrete crushing and the formation of splitting cracks originating from the high bearing stresses at the ribs of the reinforcing bars. Examples of reinforcing bars subjected to this type of loading are found in beam-column joints subjected to seismic loading. Fully reversed cyclic loading (force controlled; refer to Fig. 10(b)) was used to simulate this situation. It is noted that while the test conducted in this study can be used to evaluate the bond performance under reversed cyclic loading, it did not represent the real behavior of reinforcing bars in a beam-column joint under displacement reversals, where inelastic bar strains and compression and tension forces in the connection will significantly affect bond performance.

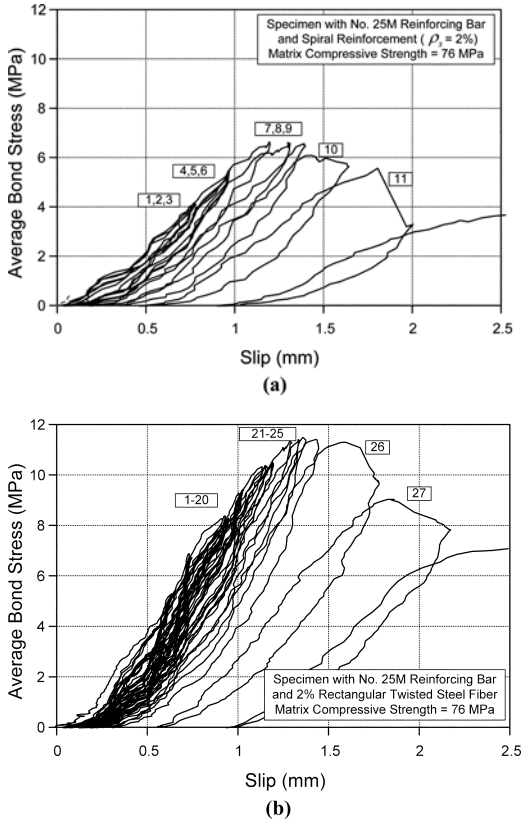

Fig. 11—Comparison of bond stress-slip responses under unidirectional force-controlled cyclic loading. (Note: number indicates the n*-th cycle; 1 mm = 0.04 in.; 1 MPa = 0.145 ksi.)*

Typical hysteresis bond stress-slip responses are shown in Fig. 12 and key test results are given in Table 5. As can be seen from Fig. 12(a), the control specimens exhibited severe degradation in bond stress and stiffness after only a few cycles. The cyclic behavior was significantly improved by using spiral reinforcement, as indicated in Fig. 12(b). Specimens with 2% UHM-PE fiber (Fig. 12(c)) showed no degradation in either bond stress or stiffness, and minor residual slip (less than 0.6 mm [0.024 in.]) in both loading directions, when the applied average bond stress demand was less than 80% of the peak monotonic bond strength. The average maximum bond stress attained in the specimens with 2% square twisted steel fibers (20 mm [0.8 in.] long) was the highest among all test specimens. This series of tests showed negligible stiffness and strength degradation when the bond stress demand reached 90% of the monotonic bond strength, with a residual slip of approximately 0.6 mm (0.024 in.). From Fig. 12(a) through (d), it can be seen that specimens with twisted steel fibers generally sustained more cycles at higher stress levels than other specimens before strength deterioration. The calculated cumulative dissipated energy through all cycles for the specimen with 2% square twisted steel fibers (20 mm [0.8 in.] long) was 22 times that of the control specimen and 2.5 times that of the spirally reinforced specimen ($\rho_s = 2\%$).

One additional series of specimens with square twisted steel fibers was tested under a force-controlled, fully reversed, low-cycle, high-amplitude fatigue test. Reversed loading cycles to a target bond stress level equal to approximately 90% of the peak monotonic bond strength (9.3 MPa [1.35 ksi]) were applied. As can be seen in Fig. 12(e), this particular specimen, with 2% fiber volume fraction, was able to sustain 26 cycles without a significant stiffness decay. It was also generally observed that under fully reversed cyclic loading, increasing fiber content from 1 to 2% by volume significantly enhanced the peak bond strength, loading cycles sustained,

Table 5—Summary of bond characteristics of specimens subjected to fully reversed, force-controlled cyclic loading (No. 25 bar and matrix compressive strength equals 76 MPa)

Fiber or reinforcement	*a*	*b*	*c*	*d*	*e*
Control	9	1.4 (60%)	1.9	4 (1.5)	54
1% PVA 13, 12 mm	14	3.5 (80%)	3.9	12 (3.9)	241
Steel spiral, ρ_s = 2%	15	7.4 (95%)	7.4	5 (5.0)	451
1% hooked, 30 mm	6	4.1 (50%)	4.5	4 (4.5)	233
2% hooked, 30 mm	21	7.4 (90%)	8.2	4 (5.4)	1014
1% UHM-PE, 38 mm	11	7.2 (70%)	8.3	4 (6.7)	1045
2% UHM-PE, 38 mm	11	8.9 (82%)	8.9	7 (8.8)	996
1% rectangular twisted, 30 mm	15	6.1 (80%)	6.9	13 (6.9)	383
2% rectangular twisted, 30 mm	23	7.6 (80%)	10.1	13 (6.9)	738
1% square twisted, 30 mm	15	6.6 (80%)	7.4	7 (6.6)	912
1% square twisted, 20 mm	9	4.3 (65%)	5.3	6 (4.3)	234
2% square twisted, 20 mm	20	9.2 (90%)	10.3	8 (8.3)	1150
2% square twisted, 20 mm*	26	9.3 (90%)	9.3	—	1313

*Constant bond stress (9.3 MPa) for 26 cycles until strength dropped.
Note: *a* is number of load cycles performed; *b* is bond stress reached, MPa, at which only minor strength, stiffness, and residual slip occur (as well as percentage of peak monotonic bond stress); *c* is peak bond stress under fully reversed, forced-controlled cyclic loading, MPa; *d* is cycle where first visible crack was observed (and corresponding bond stress, MPa; *e* is cumulative energy (N-m); 1 mm = 0.04 in.; 1 MPa = 0.145 ksi, and 1 N-m = 0.737 in.-ft.

and cumulative dissipated energy while reducing residual slip and crack width.

The superior behavior observed in reinforcing bars embedded in strain-hardening FRC composites, compared to those with typical polymeric fibers such as the PVA fibers used in this study or spiral reinforcement, can be explained as follows. In concrete members confined by transverse reinforcement such as a spiral or rectangular hoops, a minimum lateral expansion is required (leading to cracking) in the cementitious matrix before the transverse reinforcement becomes effective in providing confinement. A similar situation occurs in FRC composites with fibers of relatively low elastic modulus (compared to steel), such as PVA fibers; their tensile strength will not be used until some appreciable strain level or crack width is achieved in the cementitious matrix. These initial cracks may reduce the bond contribution from friction and mechanical interlocking, especially under reversed cyclic loading. On the other hand, the crack bridging resistance of steel fibers, such as hooked or twisted steel fibers, can be activated much earlier than that of polymeric

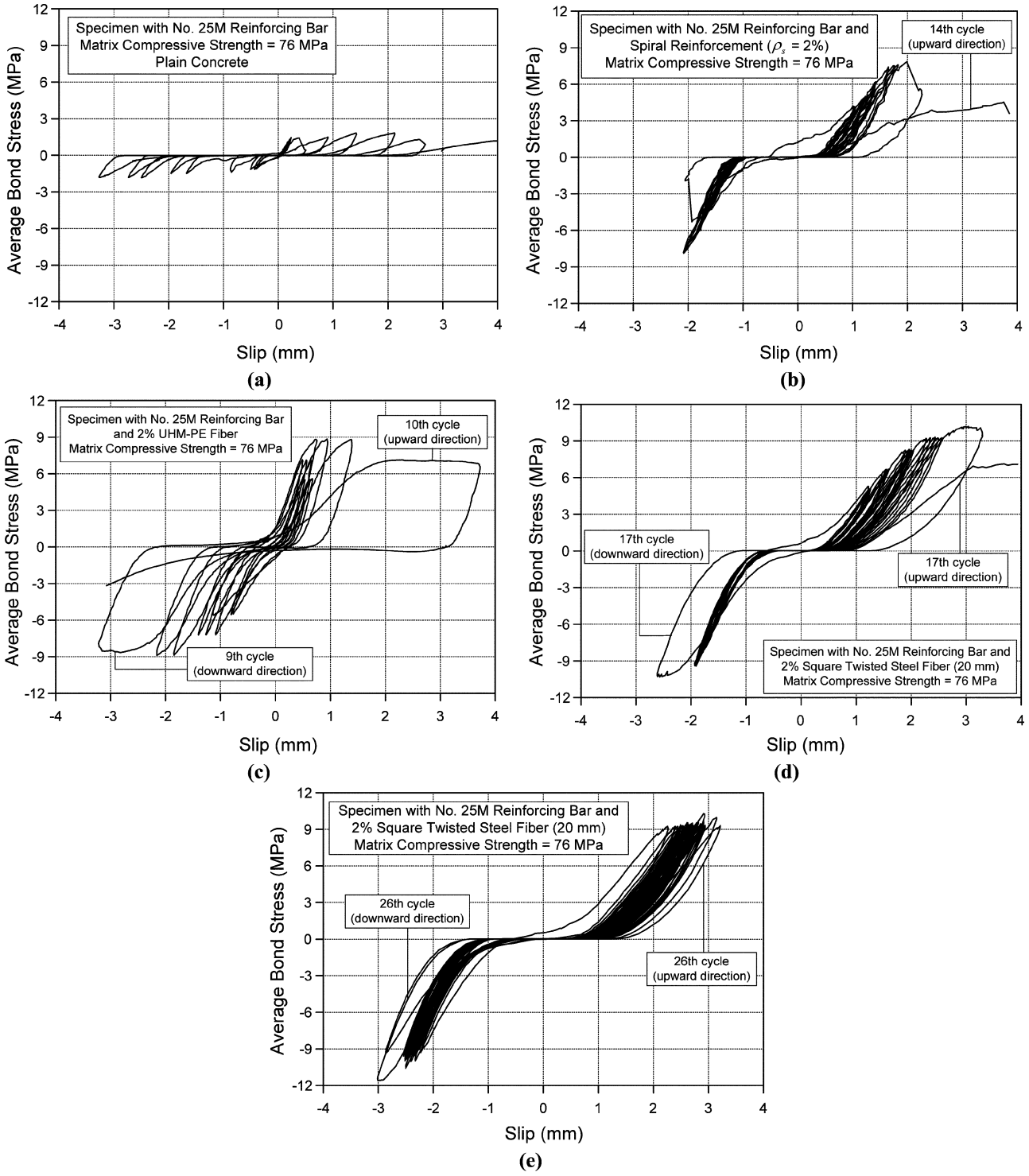

Fig. 12—Comparison of bond stress-slip responses under fully reversed, force-controlled cyclic loading. (Note: 1 mm = 0.04 in.; 1 MPa = 0.145 ksi.)

fibers due to the higher elastic modulus and bond modulus of steel fibers, which makes FRC composites with steel fibers more effective for controlling crack growth and for energy-dissipation at early loading stages.

SUMMARY AND CONCLUSIONS

The bond behavior of reinforcing bars embedded in various types of FRC composites was experimentally investigated. Both strain-hardening (or high-performance) fiber-reinforced cement composites (HPFRCCs) and strain-softening FRC composites were evaluated. The test specimens consisted of a reinforcing bar embedded in a cement composite prism subjected to monotonic, unidirectional cyclic, or reversed cyclic loading. The following conclusions can be drawn from the results of this research:

1. The confinement and bridging effects provided by fibers in FRC composites after cracking can effectively limit crack width, thereby leading to enhanced bond resistance of reinforcing bars embedded in such composites, compared to plain concrete matrixes. Specimens using tensile strain-hardening FRC composites (or HPFRCCs) led to the best bond performance in terms of bond strength and stiffness retention capacity, as well as damage-control ability.

2. Bond strength in HPFRCC specimens subjected to monotonic loading was as high as 1.5 times that of the spirally reinforced specimens. Therefore, with the same reinforcement amount (volume fraction), fibers in HPFRCCs are more effective than conventional transverse reinforcement for enhancing bond strength, as well as for crack control.

3. Bond performance of specimens with conventional spiral reinforcement (ρ_s = 2%) was inferior to that of HPFRCC specimens under unidirectional cyclic loading. The bond stress level reached was smaller (approximately 60% of that of the 2% fiber content specimens) and the residual slip was over five times greater at the same stress levels. The number of loading cycles that HPFRCC specimens sustained without bond stiffness degradation was approximately three times that of the spirally reinforced specimens. Spalling and fracturing of concrete contributed to the inferior bond performance of specimens with spirals.

4. Bond performance of reinforcing bars under fully reversed cyclic loading can also be significantly enhanced by using HPFRCC materials. Cumulative energy dissipated by the HPFRCC specimen was approximately 22 times that of the plain concrete specimen and 2.5 times that of the spirally reinforced specimen (ρ_s = 2%). HPFRCC specimens sustained a bond stress of approximately 10 MPa (1.45 ksi) over 20 fully reversed loading cycles (No. 25M [No. 8] bar), while experiencing relatively small residual slip, crack width, and overall damage.

5. Test results suggest that application of HPFRCCs can largely reduce the development length of deformed bars in reinforced concrete members.

ACKNOWLEDGMENTS

The research described herein was sponsored by the National Science Foundation under Grant No. CMS 0408623. The opinions expressed in this paper are those of the authors and do not necessarily reflect the views of the sponsor.

REFERENCES

ACI Committee 318, 2008, "Building Code Requirements for Structural Concrete (ACI 318-08) and Commentary," American Concrete Institute, Farmington Hills, MI, 473 pp.

ACI Committee 408, 2003, "Bond and Development of Straight Reinforcing Bars in Tension (ACI 408R-03)," American Concrete Institute, Farmington Hills, MI, 49 pp.

Balaguru, P.; Gambarova, P. G.; Rosati, G. P.; and Schumm, C. E., 1996, "Bond of Reinforcing Bars and Prestressing Tendons in HPFRCC Matrices," *High-Performance Fiber-Reinforced Cement Composites 2*, Proceedings of the Second International RILEM Workshop, pp. 349-381.

Chao, S.-H., 2005, "Bond Characterization of Reinforcing Bars and Prestressing Strands in High Performance Fiber Reinforced Cementitious Composites under Monotonic and Cyclic Loading," PhD dissertation, University of Michigan, Ann Arbor, MI, 475 pp.

Chao, S.-H.; Naaman, A. E.; and Parra-Montesinos, G. J., 2006, "Bond Behavior of Strands Embedded in Fiber Reinforced Cementitious Composites," *PCI Journal*, V. 51, No. 6, Nov.-Dec., pp. 56-71.

Eligehausen, R.; Popov, E. P.; and Bertero, V. V., 1983, "Local Bond Stress-Slip Relationships of Deformed Bars Under Generalized Excitations," *Report* No. UCB/EERC-83/23, Earthquake Engineering Research Center, University of California, Berkeley, Berkeley, CA, Oct.

Goto, Y., 1971, "Cracks Formed in Concrete around Deformed Tension Bars," ACI JOURNAL, *Proceedings* V. 68, No. 4, Apr., pp. 244-251.

Hota, S. R., and Naaman, A. E., 1997, "Bond Stress-Slip Response of Reinforcing Bars Embedded in FRC Matrices Under Monotonic and Cyclic Loading," *ACI Structural Journal*, V. 94, No. 5, Sept.-Oct., pp. 525-537.

Li, V. C.; Wu, H.-C.; and Chan, Y.-W., 1996, "Effect of Plasma Treatment of Polyethylene Fibers on Interface and Cementitious Composite Properties," *Journal of the American Ceramic Society*, V. 79, No. 3, Mar., pp. 700-704.

Naaman, A. E., and Reinhardt, H. W., 1996, "Characterization of High Performance Fiber Reinforced Cement Composites—HPFRCC," *High Performance Fiber Reinforced Cement Composites 2*, Proceedings of the Second International RILEM Workshop, Ann Arbor, MI, pp. 1-24.

Naaman, A. E., 2003, "Strain Hardening and Deflection Hardening Fiber Reinforced Cement Composites," *High-Performance Fiber-Reinforced Cement Composites 4*, Proceedings of the Fourth International RILEM Workshop, pp. 95-113.

Orangun, C. O.; Jirsa, J. O.; and Breen, J. E., 1977, "A Reevaluation of Test Data on Development Length and Splices," ACI JOURNAL, *Proceedings* V. 74, No. 3, Mar., pp. 114-122.

Parra-Montesinos, G. J., 2005, "High-Performance Fiber-Reinforced Cement Composites: An Alternative for Seismic Design of Structures," *ACI Structural Journal*, V. 102, No. 5, Sept.-Oct., pp. 668-675.

Sujivorakul, C., 2002, "Development of High Performance Fiber Reinforced Cement Composites Using Twisted Polygonal Steel Fibers," PhD dissertation, University of Michigan, Ann Arbor, MI, 330 pp.

Viawathanatepa, S.; Popov, E. P.; and Bertero, V. V., 1979, "Effects of Generalized Loadings on Bond of Reinforcing Bars Embedded in Confined Concrete Blocks," *Report* No. UCB/EERC-79/22, Earthquake Engineering Research Center, University of California, Berkeley, Berkeley, CA, Aug.